Characterization of solid catalysts by ^{17}O solid-state NMR

Spectroscopic background: ^{17}O nuclei have a spin of I = 5/2 and a quadrupole moment of Q = -2.558 x 10^{-30} m^2. Therefore, ^{17}O NMR signals of oxygen atoms in solids are affected by quadrupolar interactions. Due to the low natural abundance of the ^{17}O isotope of 0.037 % and the sensitivity in comparison with ^{1}H nuclei (1.0) of 1.1 x 10^{-5} only, ^{17}O solid-state NMR spectroscopy of catalysts requires an isotopic enrichment. For basic principles of solid-state NMR, see lectures “Solid-State NMR Spectroscopy” for Bachelor students or PhD seminars, accessible via the link “Lectures for Students”.

Early ^{17}O broad-line NMR spectroscopic studies of water-free aluminosilicate-type zeolites, performed without the application of MAS, led to broad quadrupole patterns corresponding to a quadrupole coupling constant of about C_Q **= 4.6-5.2 MHz** and **3.1 to 3.2 MHz** due to oxygen atoms in **Si-O-Si** and **Si-O-Al bridges**, respectively. The isotropic chemical shifts were determined to $\delta_{17O,iso}$ **= 44 to 57 ppm for Si-O-Si** and **31 to 45 ppm for Si-O-Al** bridges [1]. Simulation of the ^{17}O broad-line NMR spectra of **aluminophosphates** gave C_Q **= 5.6-6.5 ppm** and $\delta_{17O,iso}$ **= 61 to 67 ppm for Al-O-P** bridges. **Gallosilicates** contain **Si-O-Ga** bridges with C_Q **= 4.0 to 4.8 ppm** and $\delta_{17O,iso}$ **= 28 to 29 ppm** [2].

Nowadays, ^{17}O solid-state NMR investigations of catalysts are performed applying the MAS, DOR, and two-dimensional (2D) MQMAS techniques [3-8]. A prerequisite for obtaining well-resolved ^{17}O MAS, DOR, and 2D MQMAS NMR spectra is the presence of ordered local structures, such as those occurring in siliceous zeolites and in zeolites with an alternating arrangement of silicon and aluminum atoms at T-

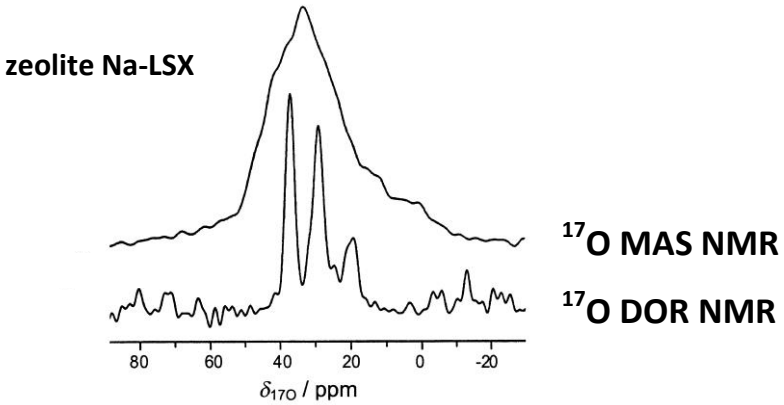

Fig. 1

positions (n_{Si}/n_{Al} = 1). In these cases, the different signals of oxygen atoms at crystallographically non-equivalent O-sites appear as well-resolved signals in the ^{17}O DOR NMR (**Fig. 1**) and ^{17}O MQMAS NMR spectra (**Fig. 2**). For siliceous **zeolite FER** and utilizing ^{17}O MQMAS NMR spectroscopy, up to 10 different signals of oxygen atoms at crystallographically non-equivalent positions in Si-O-Si bridges were found [4]. While the isotropic chemical shifts of these signals cover a range of $\delta_{17O,iso}$ **= 28.0 to 43.1 ppm,** slightly different quadrupole coupling constants in the range of C_Q **= 5.2 to 5.6 MHz** were determined.

The significant effect of the DOR technique on the spectral resolution in comparison with the MAS technique for the study of quadrupolar nuclei is demonstrated in **Fig. 1** [3]. While the ^{17}O MAS NMR spectrum of ^{17}O-enriched and dehydrated zeolite Na-LSX (n_{Si}/n_{Al} = 1) consists of a single broad signal, the application of the DOR technique leads to a split of the spectrum into three narrow signals. The potential of the 2D MQMAS technique is demonstrated in **Fig. 2**, which shows the ^{17}O MQMAS NMR spectrum of oxygen atoms in zeolite Na-LSX [3]. The signals obtained along the δ_2-axis of the two-dimensional spectrum in **Fig. 2** correspond to the one-dimensional ^{17}O MAS NMR spectrum (projection on top). These signals are affected by second-order quadrupolar signal broadening. The signals obtained along the δ_{iso}-axis (projection at the left-hand side) are comparable with those in the ^{17}O DOR NMR

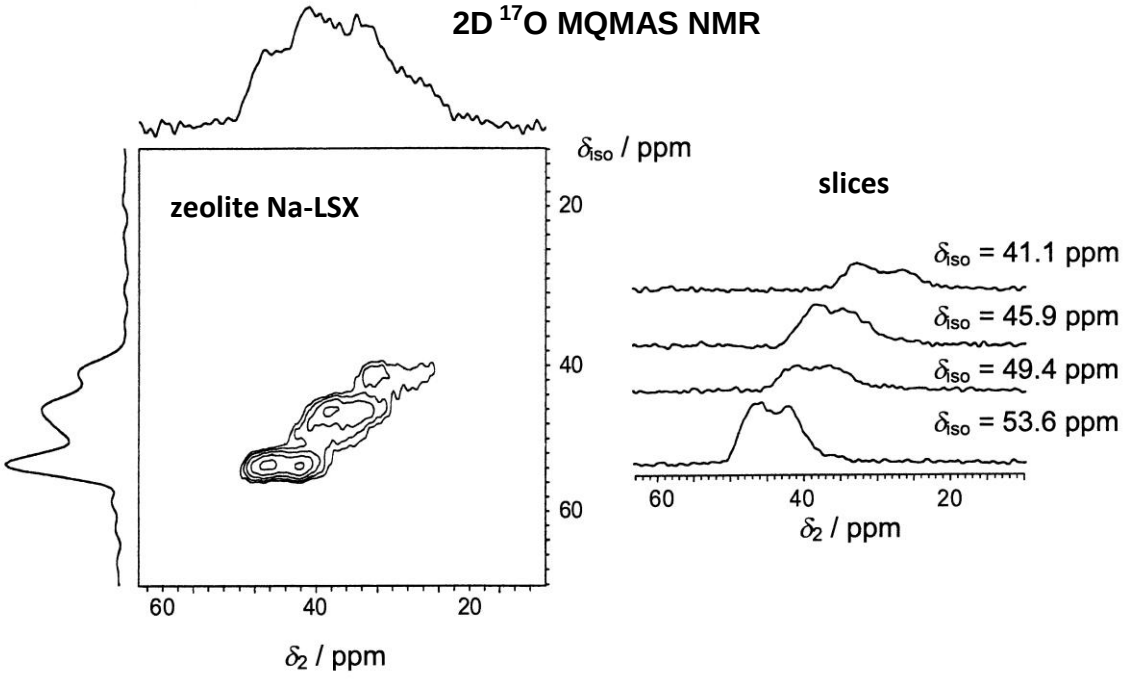

Fig. 2

spectrum in **Fig 1, bottom**. In this dimension, the anisotropic second-order quadrupolar signal broadenings are averaged by the multiple-quantum experiment. On the right-hand side of **Fig. 2**, slices cut parallel to the δ_2-axis at different δ_{iso} values are depicted. These slices correspond to the different ^{17}O MAS NMR signals of oxygen atoms at the crystallographically non-equivalent oxygen positions in **zeolite Na-LSX**. The simulation of these slices allows a determination of the quadrupole parameters of the corresponding ^{17}O nuclei and led to quadrupole coupling constants of $\boldsymbol{C_Q}$ **= 3.2 to 3.6 MHz** and chemical shifts of $\boldsymbol{\delta_{17O,iso}}$ **= 41.1 to 53.6 ppm** for oxygen atoms at the four crystallographically non-equivalent O-sites in zeolite Na-LSX [3].

Data obtained by 2D ^{17}O MQMAS NMR spectroscopy of oxygen atoms at crystallographically non-equivalent oxygen positions in zeolites Na-A and Na-LSX (both n_{Si}/n_{Al} = 1) yielded a correlation between their isotropic chemical shift $\delta_{17O,iso}$ and the Si-O-Al bond angle β [3]:

$$\delta_{17O,iso} \text{ / ppm} = -0.71\ \beta + 143.7 \qquad (1)$$

Eq. (1) can be utilized to calculate Si-O-Al bond angles β in materials, where a determination of the local oxygen structure by X-ray diffraction is not possible.

^{17}O solid-state NMR spectroscopic studies of non-crystalline powder materials are complicated by the distribution of the bond geometries in the local structure of the oxygen atoms and, therefore, of the ^{17}O quadrupole parameters. By ^{17}O spin-echo and MAS NMR experiments, the oxygen atoms in **silica,** synthesized via the sol-gel technique, were investigated [9]. The signals of oxygen atoms in the **Si-O-Si** bridges were found to be characterized by a quadrupole coupling constant of $\boldsymbol{C_Q}$ **= 5.3 MHz** and an isotropic chemical shift of $\boldsymbol{\delta_{17O,iso}}$ **= 42 ppm**. The SiOH fragments caused signals in a **wide range of** $\boldsymbol{C_Q}$ values and at isotropic chemical shifts of $\boldsymbol{\delta_{17O,iso}}$ **= 0 ± 20 ppm**. The behaviour of the latter signals is explained by the above-mentioned distribution of the bond geometries in the local structure of the **SiOH** fragments.

Titanium oxides, TiO_2, are extensively studied materials because they are widely employed as conventional catalyst supports [10], pigments [11], and photocatalysts [12, 13]. The two common phases are **anatase (A)** and **rutile (R**). The rutile phase is the most stable structure of TiO_2, while the anatase phase can transform to rutile at high temperatures. Both anatase and rutile consist of TiO_6 units, which are joined

together by sharing different numbers of edges - two in rutile and four in anatase. The photocatalytic activity of TiO_2 could be related to phase-junctions formed between the anatase and rutile domains, which enhance the hydrogen production in the photocatalytic water splitting [14, 15]. Therefore, the **$^{16/17}$O isotope exchange (OIE)** on water-free pure anatase in comparison with mixed-phase TiO_2 materials, containing anatase and rutile domains as well as various surface oxygen species and phase conjunctions on the anatase and rutile domains, was studied by ^{17}O MAS NMR spectroscopy upon a thermally induced OIE with $^{17}O_2$ gas [16]. By this way, the activation energies of the OIE were determined for the above-mentioned materials.

Fig. 3 shows the stacked plots of **^{17}O MAS NMR spectra** of **pure anatase (a, TiO_2/A)** and an **anatase/rutile mixture (b, TiO_2/A+R)** recorded upon OIE with $^{17}O_2$ gas (p = 500 mbar) at T = 773 K up to t = 80 h. The ^{17}O MAS NMR signal at **δ_{17O} = 562 ppm** is due to ^{17}O atoms in pure **anatase** and has a signal shape according to a quadrupole coupling constant of **C_Q = 1.2 MHz**. The signal at **δ_{17O} = 596 ppm**, with a similar signal shape, is caused by ^{17}O atoms in **rutile**, while surface ^{17}O atoms of the anatase/rutile **domain mixture** are responsible for the signals at **δ_{17O} = 516 ppm, 543 ppm,** and **572 ppm** [16].

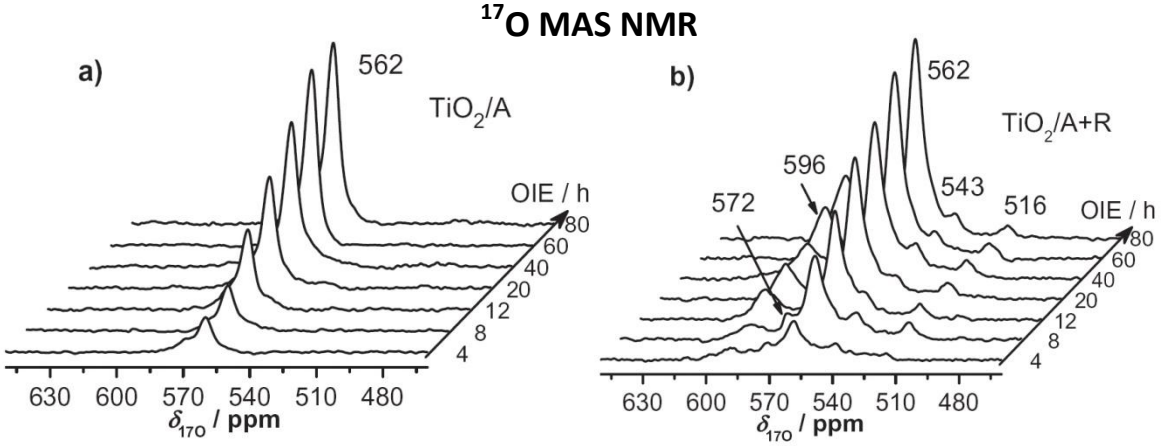

Fig. 3

The **$^{16/17}$O isotope exchange (OIE) kinetics**, investigated upon thermal treatments of the $^{17}O_2$ gas-loaded TiO_2 materials at T = 723 K, 773 K, and 823 K, led to the Arrhenius plots of the velocity constants k_i of ^{17}O atoms in the pure anatase (TiO_2/A) and in anatase/rutile domains (TiO_2/A+R) shown in **Fig. 4** [16]. These plots indicate a strong decrease of the activation energy of the OIE on the **mixed-phase TiO_2/A+R**

material (***E*****$_a$ = 61 kJ/mol** for the **anatase domains** and ***E*****$_a$ = 70 kJ/mol** for the **rutile domains**) compared with the **pure anatase** TiO_2/A material (***E*****$_a$ = 105 kJ/mol**). Furthermore, the very rapid increase of the ^{17}O MAS NMR signals of surface oxygen species on the TiO_2/A+R material indicates that the OIE starts at these surface sites, which subsequently exchange their ^{17}O atoms with ^{16}O framework atoms in anatase and rutile domains [16].

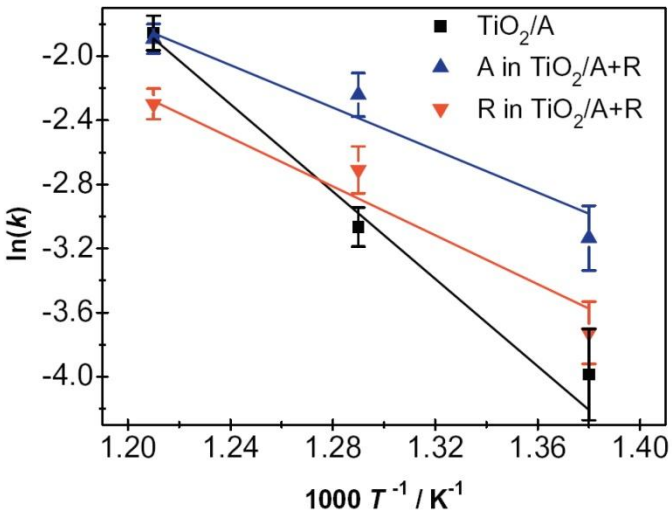

Fig. 4

For a survey on ^{17}O solid-state NMR parameters of oxygen atoms in powder materials, see Refs. [17] and [18].

Catalyst preparation: The ^{17}O enrichment of powder materials used for the NMR studies presented in Figs. 1 and 2 was performed by a treatment in a reactor with $H_2{}^{17}O$ vapour at 523 K for several hours [3]. For the studies presented in Fig. 3, the dehydrated TiO_2 materials filled in quartz glass tubes were loaded with 500 mbar $^{17}O_2$ gas. Upon sealing the quartz glass tubes, these samples were heated at T = 723 to 823 K for up to t = 80 h.

^{17}O solid-state NMR studies: ^{17}O DOR NMR experiments were performed at the Larmor frequency of ν_0 = 67.8 MHz in the magnetic field of B_0 = 11.7 T [3]. For the 2D ^{17}O MQMAS experiments, the Larmor frequency of ν_0 = 101.7 MHz and the external magnetic field of B_0 = 17.6 T were utilized [3]. The MQMAS pulse sequence

consisted of two strong pulses and an additional weak z-filter pulse [19]. A total ring down delay of 7 µs after the z-filter pulse and a repetition time of t = 200 ms were used. The non-selective nutation frequency of 100 kHz was determined for a $H_2{}^{17}O$ sample at the Larmor frequency of ν_0 = 101.7 MHz. For this rf power, the widths of the first and second pulse were adjusted for maximum signal intensity to 3.4 and 1.2 µs, respectively. The selective $\pi/2$ pulse length of the z-filter was adjusted to 50 µs [3]. The ^{17}O MAS NMR investigations of the TiO_2 materials were performed at the Larmor frequencies of ν_0 = 54.2 MHz upon single pulse excitation of $\pi/6$, with the repetition time of t = 0.5 s, and the sample spinning rate of ν_{rot} = 20 kHz using a 2.5 mm MAS NMR probe. The chemical shifts were referenced to liquid $H_2{}^{17}O$ (δ_{17O} = 0 ppm).

References:

[1] H.K.C. Timken, G.L. Turner, J.-P. Gilson, L.B. Welsh, E. Oldfield, *Solid-state oxygen-17 nuclear magnetic resonance spectroscopic studies of zeolites and related systems, Part 1*, J. Am. Chem. Soc. 108 (1986) 7231-7235, DOI: 10.1021/ja00283a017.

[2] H.K.C. Timken, N. Janes, G.L. Turner, S.L. Lambert, L.B. Welsh, E. Oldfield, *Solid-state oxygen-17 nuclear magnetic resonance spectroscopic studies of zeolites and related systems,* Part 2, J. Am. Chem. Soc. 108 (1986) 7236-7241, DOI: 10.1021/ja00283a018.

[3] U.-T. Pingel, J.-P. Amoureux, T. Anupold, F. Bauer, H. Ernst, C. Fernandez, D. Freude, A. Samoson, *High-field ^{17}O NMR studies of the SiOAl bond in solids*, Chem. Phys. Lett. 294 (1998) 345-350, DOI: 10.1016/S0009-2614(98)00847-1.

[4] L.M. Bull, B. Bussemer, T. Anupold, A. Reinhold, A. Samoson, J. Sauer, A.K. Cheetham, R. Dupree, *A high-resolution ^{17}O and ^{29}Si NMR study of zeolite siliceous ferrierite and ab initio calculations of NMR parameters*, J. Am. Chem. Soc. 122 (2000) 4948-4958, DOI: 10.1021/ja993339y.

[5] D. Freude, T. Loeser, D. Michel, U. Pingel, D. Prochnow, *^{17}O NMR studies of low silicate zeolites*, Solid State Nucl. Magn. Reson. 20 (2001) 46-60, DOI: 10.1006/snmr.2001.0029.

[6] J.E. Readman, N. Kim, M. Ziliox, C.P. Grey, *^{17}O MQMAS NMR studies of Na-A and Ca-A*, Chem. Commun. (2002) 2808-2809, DOI: 10.1039/b208356f.

[7] T. Loeser, D. Freude, G.T.P. Mabande, W. Schwieger, *^{17}O NMR studies of sodalites*, Chem. Phys. Lett. 370 (2003) 32-38, DOI: 10.1016/S0009-2614(03)00066-6.

[8] J.E. Readman, C.P. Grey, M. Ziliox, L.M. Bull, A. Samoson, *Comparison of the ^{17}O NMR spectra of zeolites LTA and LSX*, Solid State Nucl. Magn. Reson. 26 (2004) 153-159, DOI: 10.1016/j.ssnmr.2004.03.004.

[9] E.R.H. van Eck, M.E. Smith, S.C. Kohn, *Observation of hydroxyl groups by ^{17}O solid-state multiple quantum MAS NMR in sol-gel-produced silica*, Solid State Nucl. Magn. Reson. 15 (1999) 181-188, DOI: 10.1016/S0926-2040(99)00055-7.

[10] M.C.J. Bradford, M.A. Vannice, *Catalytic reforming of methane with carbon dioxide over nickel catalysts,* Appl. Catal. A: Gen. 142 (1996) 73-96, DOI: 10.1016/0926-860X(96)00065-8.

[11] G. Pfaff, P. Reynders, *Angle-dependent optical effects deriving from submicron structures of films and pigments*, Chem. Rev. 99 (1999) 1963-1981, DOI: 10.1021/cr970075u.

[12] A. L. Linsebigler, G. Q. Lu, J. T. Yates, *Photocatalysis on TiO_2 surfaces: Principles, mechanisms, and selected results*, Chem. Rev. 95 (1995) 735-758, DOI: 10.1021/cr00035a013.

[13] X. Sun, W. Dai, G. Wu, L. Li, N. Guan, M. Hunger, *Evidence of rutile-to-anatase photo-induced electron transfer in mixed-phase TiO_2 by solid-state NMR spectroscopy*, Chem. Commun. 51 (2015) 13779-13782, DOI: 10.1039/c5cc04971g.

[14] J. Zhang, Q. Xu, Z. Feng, M. Li, C. Li, *Importance of the relationship between surface phases and photocatalytic activity of TiO_2*, Angew. Chem. Int. Ed. 47 (2008) 1766-1769, DOI: 10.1002/anie.200704788.

[15] J. Zhang, Q. Xu, M. Li, Z. Feng, C. Li, *UV Raman spectroscopic study on TiO_2. II. Effect of nanoparticle size on the outer/inner phase transformations*, J. Phys. Chem. C 113 (2009) 1698-1704, DOI: 10.1021/jp808013k.

[16] X. Sun, M. Dyballa, J. Yan, L. Li, N. Guan, M. Hunger, *Solid-state NMR investigation of the $^{16/17}O$ isotope exchange of oxygen species in pure-anatase and mixed-phase TiO_2*, Chem. Phys. Lett. 594 (2014) 34-40, DOI: 10.1016/j.cplett.2014.01.014.

[17] D. Freude, *Quadrupolar Nuclei in Solid-State Nuclear Magnetic Resonance*, in: Encyclopedia of Analytical Chemistry: Applications, Theory, and Instrumentation, Wiley, 2006, DOI: 10.1002/9780470027318.a6112.

[18] D. Freude, https://www.dieter-freude.de/quad-nmr.

[19] J.-P. Amoureux, C. Fernandez, S. Steuernagel, *Z filtering in MQMAS NMR*, J. Magn. Reson. A 123 (1996) 116-118, DOI: 10.1006/jmra.1996.0221.